

Evaluating a novel bidirectional soft-switching DC-DC converter for electric vehicles

Prasannakumar Inampudi¹, P. Chandrasekar¹, T. Vijay Muni²

¹Department of Electrical and Electronics Engineering, Vel Tech Rangarajan Dr. Sagunthala R&D Institute of Science and Technology, Chennai, India

²Department of Electrical and Electronics Engineering, Koneru Lakshmaiah Education Foundation, Vaddeswaram, India

Article Info

Article history:

Received Oct 3, 2023

Revised Mar 26, 2024

Accepted Apr 26, 2024

Keywords:

DC-DC converter

High gain

MPPT

PWM

Solar PV system

Zeta converter

ABSTRACT

This research aims to build unique zero voltage transition (ZVT) non-isolated bidirectional DC-DC converters for hybrid electric vehicle battery storage. First, a high-voltage gain bidirectional converter (BDC) is examined. This converter can soft-switch insulated gate bipolar transistors (IGBTs). The primary insulated-gate bipolar transistors (IGBTs) are operated under zero-current conditions throughout the turn-on to turn-off commutation phase to reduce switching losses and increase efficiency. A soft-switched cell with a resonant inductor, capacitor, and additional IGBTs achieves zero-current turn-off. A new converter uses insulated-gate bipolar transistors with zero-voltage transition operation. Soft-switched cells improve the hard-switched bridgeless DC-DC converter (BDC). Resonant inductors, capacitors, and auxiliary switching devices make up the soft-switched cell. Soft-switched cells enable zero voltage turn-on of primary insulated-gate bipolar transistors. This converter charges the battery in buck mode and boosts it to provide the necessary output voltage. This study examined a 70 V/300 V power system's high-gain bidirectional converter (BDC) design simulation. The converter was tested at 50 kHz with 800 W output power. The high-gain soft-switched BDC has 96.5% boost and 97% buck efficiency. Operating principles, design analysis, and simulation assessments are included in this study.

This is an open access article under the [CC BY-SA](https://creativecommons.org/licenses/by-sa/4.0/) license.



Corresponding Author:

Prasannakumar Inampudi

Department of Electrical and Electronics Engineering

Vel Tech Rangarajan Dr. Sagunthala R&D Institute of Science and Technology

Chennai, Tamil Nadu 600062, India

Email: iprasannakumar.phd@gmail.com

1. INTRODUCTION

The usage of DC-DC converters is greatly improving battery storage applications. The easiest way to choose an efficient converter for industrial applications is to develop topologies that take factors like efficiency and switching power losses into account. These variables will increase the performance of the converters. These are also the features that will make these converters work better. The use of soft-switched bidirectional converters in battery storage devices (such fuel cells and supercapacitors) is the primary focus of ongoing research in this area. A zero-voltage transition for a DC-DC boost converter has been the focus of prior research on auxiliary resonant switches [1]. Using linked inductors, self-commutation, and an auxiliary cell, the soft-switched bidirectional converters [1]-[6] were constructed. Battery chargers that are engineered to run with very low output power levels while preserving a high degree of efficiency are ideal for use with these soft-switched bidirectional converters [7]-[12]. The zero current switching activity of the switches is

likewise the center of attention in this work, similar to how zero voltage transition (ZVT) is. With the help of supplementary resonant cells [13] and a high voltage gain zero voltage switching isolated DC-DC converter [14], these switches were developed for use in battery storage applications. The soft-switching was also made possible by the inclusion of an additional snubber capacitor and leakage inductance in the main power supply insulated-gate bipolar transistors (IGBTs). Within the context of energy storage system applications in electric vehicles, this chapter presents a new ZVT bidirectional DC-DC converter as a practical solution. This application's background is described in the preceding phrase.

Research that followed focused on creating compact, inexpensive, and non-isolated converters for backup battery systems. In order to facilitate soft switching operations at the switching devices and diodes of non-isolated, high-voltage-gain boost converters, a passive resonant circuit was included into their design [15]-[18]. Maintaining a resonance frequency lower than the working frequency allowed them to accomplish soft-commutation zero-voltage transitions (ZVTs) in both diodes and MOSFETs. For the secondary power supply systems of electric cars, the group shifted its attention to developing non-isolated bidirectional DC-DC converters [19]. These converters rely on basic series resonant components to enable zero-voltage switching (ZVS) turn-on of the primary switching devices. The use of a voltage multiplier cell and a parallel resonant circuit inductor-capacitor (LCC) allowed for the construction of non-isolated high-gain boost converters [20]. They used zero-voltage (ZV) action to turn on the diodes and zero-current (ZC) action to turn on the main switches. Despite the fact that very low power and a very high switching frequency (150 kHz) produced very poor efficiency. Nonetheless, a current-fed unidirectional converter was developed without voltage multiplier cells [21], [22]. This converter achieved an efficiency of 95.5% at operating frequencies greater than 100 kHz and had ZC turn-off operations for its switches. Zhang and Chau [16] state that in soft-switching situations, several non-isolated type converter topologies are applicable. Engineers at MIT developed a voltage-free passive lossless bidirectional converter (BDC) [23] to enable electromechanical braking systems in electric cars without internal combustion engines. Reducing the input voltage (V_{in}), input power, and switching frequency is not given much attention [24]-[26]. On the other hand, at very low output power levels, it has achieved an efficiency of around 94%.

The suggested converter is capable of operating in either a boost or buck mode depending on the situation. This work proposes using a novel kind of converter that is not isolated from the rest of the circuit in order to bring about the desired transition of zero voltage to the primary switches. This converter would make use of resonant components and operate in concert with active auxiliary devices. The key advantages that this converter may provide are an increased level of efficiency as well as a reduction in the amount of turn-on losses.

2. DESCRIPTION OF PROPOSED BIDIRECTIONAL DC-DC CONVERTER

The schematic diagram represents a bidirectional DC-DC converter as shown in Figure 1. In this configuration, the primary switches $S1$ and $S2$ can independently transfer power in both directions, enabling the converter to operate in either boost or buck mode. Additionally, components like inductors $L1$ and $L2$ capacitors $C1$, $C2$, and $C3$ and the input voltage sources $V1$ and $V2$ are integrated into the circuit to facilitate energy transfer and regulate voltage levels across the system. Switches Sa and Sb play a role in controlling the current path, ensuring efficient power conversion and management within the circuit.

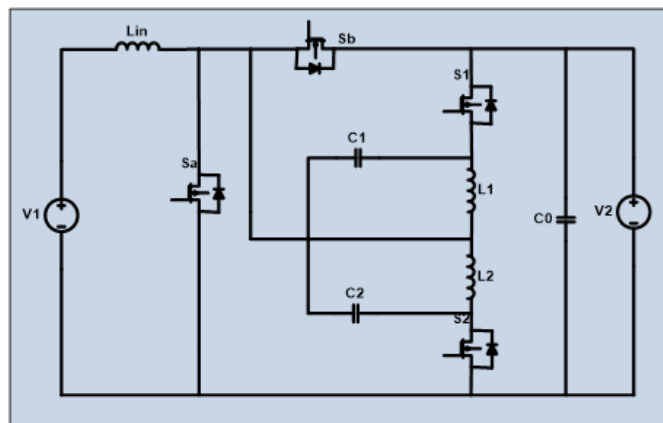


Figure 1. Proposed new ZVT bidirectional DC-DC converter

The key waveforms of the proposed converter were shown in Figure 2. The operating concept was explained with the use of representations of current flow that were shown in Figure 3 for the boost mode, and Figure 4 illustrated the schematics for the buck mode. Reduced power consumption during the turn-on process of the primary active devices, as well as reduced power consumption during the switching process of the secondary active devices.

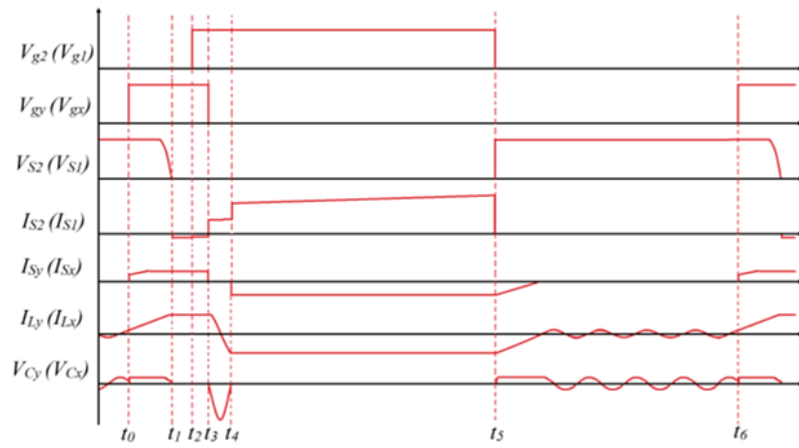


Figure 2. Key waveforms: boost and buck modes

3. PRINCIPLES OF OPERATION AND ITS ANALYSIS

3.1. Boost mode operation

Figure 2 depicts the usual voltage and current waveforms for the length of one switching cycle (from t_0 to t_6) and demonstrates how the corresponding current flow models of the boost mode are depicted in the figure. This converter may function in a total of six different topological modes, which are shown from a to d in Figure 3, and are broken down into the following categories.

- Mode 1: IGBT S2 is switched on at time t_0 in order to ensure zero voltage turn-on for IGBT Sa, which takes place later. The voltage between the collector and the emitter drops in a sinusoidal pattern as it approaches zero; this can be seen quite clearly in Figure 3 as the main waveforms. At the conclusion of this time period t_1 , the voltage has dipped to zero, and current in the opposite direction is flowing via the anti-parallel diode of the IGBT Sa. The following equation may be used to represent the current and voltage of an inductor with the symbol L_2 and a capacitor with the symbol C_2 :

$$i_{L2}(t_2) = I_{in}(t) + \frac{V_0}{Z} \sin w(t - t_1) \quad (1)$$

$$V_{C2}(t) = V_0 \cos w(t - t_1) \quad (2)$$

$$\omega = \frac{1}{\sqrt{L_2 C_2}}$$

$$Z = \sqrt{\frac{L_2}{C_2}}$$

- Mode 2: During the time between t_1 and t_2 , the auxiliary IGBT S2 and the diode of Sa are conducting. The diode of Sa provides the current flow channel for the resonant current that is created by L_2 and C_2 when the freewheeling mode is active as shown in Figure 4. Current and voltage expressions for an inductor with the symbol L_2 and a capacitor with the symbol C_2 are defined as:

$$i_{L2}(t_2) = I_{min} \frac{V_1}{L}(t - t_2) \quad (3)$$

$$V_{C2}(t_2) = 0 \quad (4)$$

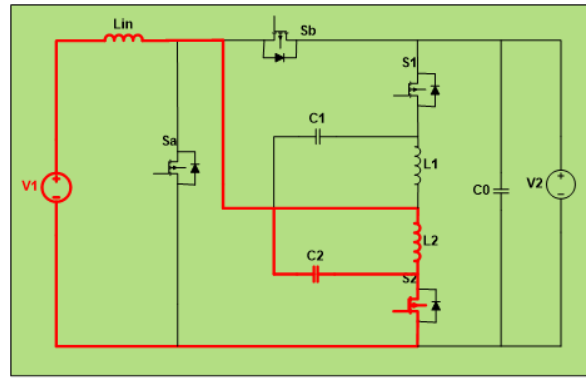


Figure 3. Current flow equivalent circuit for time interval (t0-t1) - boost mode

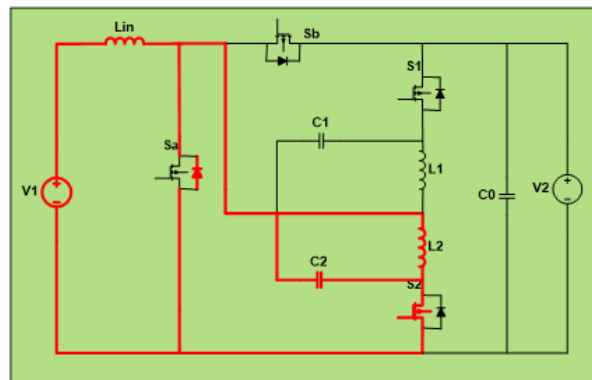


Figure 4. Current flow equivalent circuit for time interval (t1-t2) and for a time interval (t2-t3) - boost mode

- Mode 3: Since the diodes of the IGBT Sa and S2 have been conducted during the preceding time intervals, the gate pulses are applied to Sa at the moment t2 when the timing sequence begins. During this phase of freewheeling, the diode of Sa provides the channel for the resonant current to follow as shown in Figure 4. Current and voltage expressions for an inductor with the symbol L2 and a capacitor with the symbol Cy are defined as:

$$i_{L2}(t) = I_{L2}(t_3) + \frac{V_0}{Z} \cos \omega (t - t_4) \quad (5)$$

$$V_{C2}(t_3) = -Z i_{L2}(t_3) \sin \omega (t) \quad (6)$$

$$V_{C2}(t_4) = 0 \quad (7)$$

- Mode 4: From time point t3 until time point t4, the current that flows through the main switch Sa is equal to the output current, while the current that flows through the auxiliary switch is zero as shown in Figure 5. The following is the definition of the expression for the inductor L2 current:

$$i_{L2}(t) = I_{in} + \frac{V_1}{L} (t - t_4) \quad (8)$$

$$i_{L2}(t) = i_{L2}(t_4) \quad (9)$$

- Mode 5: From the t4 to t5 period, there is a current flow in the opposite direction via the auxiliary switch diode, while the current is flowing normally through the main switch. While in this accumulating mode, the input inductor Lin is allowed to build up its total value as shown in Figure 5.
- Mode 6: Because there is output current flow by the energized input inductor Lin during the period t5-t6, all of the switching devices are switched off at this time. Throughout the duration of this powering mode, the output power is transferred via Sb's L-body diode as shown in Figure 6.

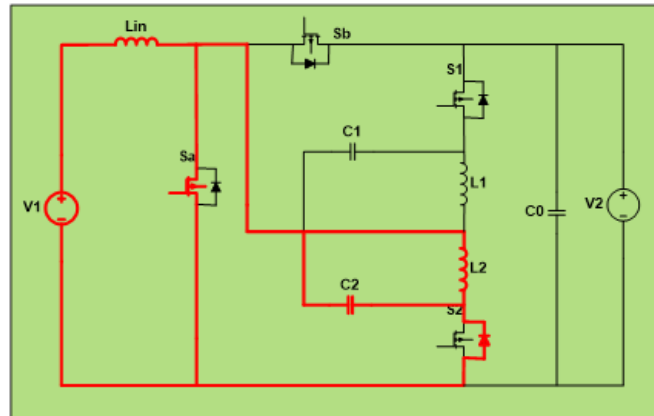


Figure 5. Current flow equivalent circuit for time interval (t_3 - t_4) and for time interval (t_4 - t_5) - boost mode

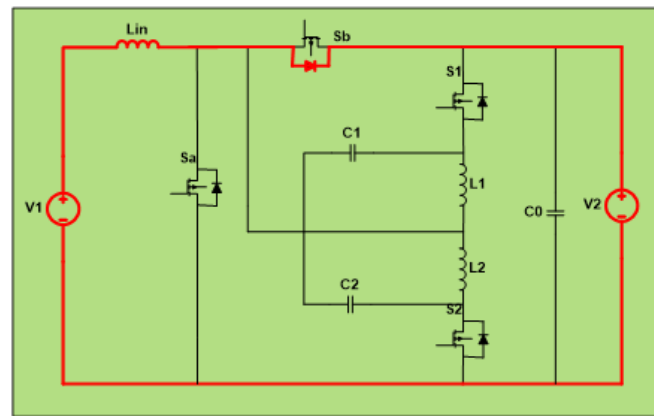


Figure 6. Current flow equivalent circuit for time interval (t_5 - t_6) - boost mode

3.2. Buck mode operation

As seen in Figure 2, the buck mode functioning may be broken down into six distinct topological modes. These modes are determined by the normal voltage and current waveforms. Figures 7-10 provide visual representations of the corresponding operating models. Whenever this mode is active, the S_b is functioning as the power transfer switch, and the S_1 has the capability of functioning as an auxiliary switch. However, in order to prevent the main IGBT from being gated, the auxiliary switch can only be used for a very short period of time before it becomes inoperable. The following is a description of each of the six distinct topological modes:

- Mode 1: The supplementary IGBT S_1 is switched on at time t_0 in order to ensure gentle turn-on for the IGBT S_b , which occurs later. The auxiliary inductor L_1 and the auxiliary inductor C_1 are resonating with one another as shown in Figure 7. During this resonant phase, the voltage of the switch gradually goes from one value to the next until it reaches zero at time t_1 .
- Mode 2: During this freewheeling mode, at the time t_1 , the diode of S_b begins conducting in order to create a free-wheeling channel in order to enable resonant tank current, which is provided by L_1 , C_1 as shown in Figure 8. The level of the output current is reached by the current via the resonant inductor, L_1 .
- Mode 3: Beginning at time t_2 , the diode of switch S_2 continues to conduct, while gating signals are also being applied to switch S_1 at the same time. When this time period t_2 has passed, the diode of S_a will have been switched off, but the output current level will have been maintained by the inductor current as shown in Figure 8.
- Mode 4: At time t_3 , the auxiliary IGBT S_1 is shut off, which results in the current flowing through it being zero. The primary IGBT S_b begins conducting, and an output power flow may be seen through the S_b - L_{in} connection as shown in Figure 9. During this mode of powering, the current flowing through the inductor L_1 linearly falls until it reaches zero, and the resonant capacitor C_1 is charged to the level of the input voltage before being discharged at t_4 .

- Mode 5: During this powering mode, the IGBT Sb is conducting from t_4 to t_5 , and the diode of S1 offers a freewheeling channel for the resonant tank current. Throughout the whole of this time, the output power is transferred to the resistance R by way of the V2-Sb-Lin circuit. At time t_5 , both the diode of S1 and the IGBT Sb are switched off as shown in Figure 10.
- Mode 6: From t_5 - t_6 , all the switches are turned-off. Therefore, there is no power to be delivered to the load.

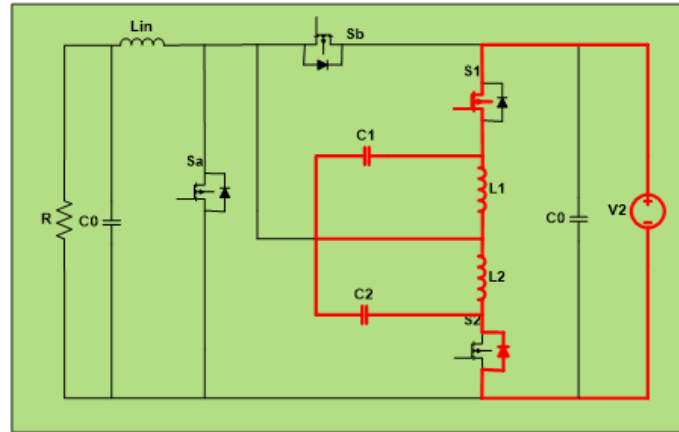


Figure 7. Current flow equivalent circuit for time interval (t_0 - t_1) - buck mode

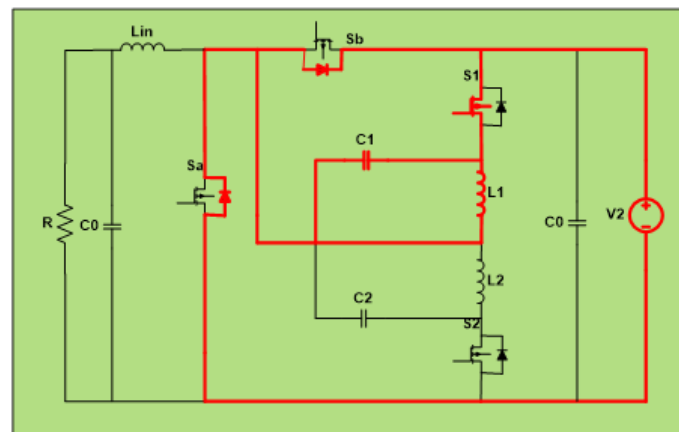


Figure 8. Current flow equivalent circuit for time interval (t_1 - t_2) and for time interval (t_2 - t_3) - buck mode

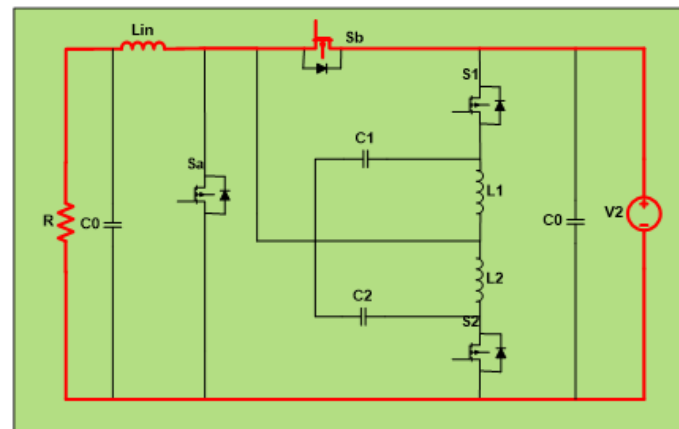


Figure 9. Current flow equivalent circuit for time interval (t_3 - t_4) - buck mode

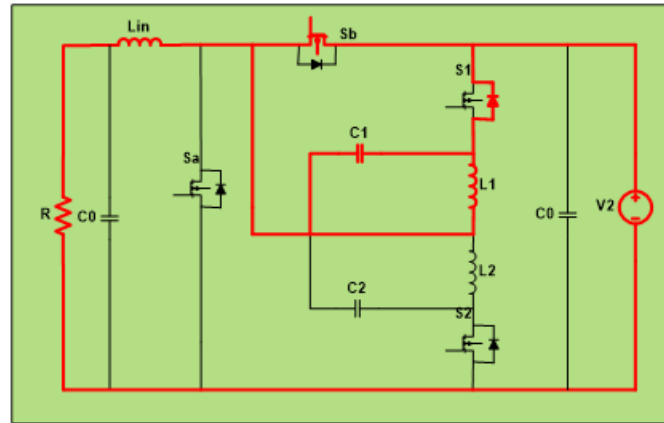


Figure 10. Current flow equivalent circuit for time interval (t4-t5) - buck mode

4. DESIGN ANALYSIS

The auxiliary resonant elements L_y , C_y are defined as a function of the current stress on the auxiliary IGBT, given by $Y1$ which is directly related to conduction losses, it is chosen less than the value 1.244 in this converter.

$$Y_1 = \left[1 + \left(\frac{V_0}{Z I_{in}} \right) \right] \quad (10)$$

The total soft-commutation (ZVT) time is given by t_{ZVT} .

$$t_{ZVT} = \frac{I_{in} L_2}{V_1} + \frac{\pi \sqrt{L_2 C_2}}{2} \quad (11)$$

By solving the (9) and (10) for L_y and C_y , the following expressions can be found:

$$L_2 \leq \frac{V_0 t_{ZVT}}{I_0 \left(1 + \frac{\pi(Y_1 - 1)}{2} \right)} \quad (12)$$

$$C_2 \leq \frac{L_2 \left(1 + \frac{V_1}{Z} \right)^2}{V_1^2} \quad (13)$$

In Table 1, the input and output parameters of the converter are presented for your perusal. The value of $Y1$ determines which numerical solution to use for the (11) and (12), respectively. The value of $Y1$ is determined to be 1.244, and the time period soft-transition (ZVT) is set to 10%; the values of resonant inductors $L1$, $L2$ are obtained as 5 H based on (11), and the values of resonant capacitors $C1$, $C2$ may be chosen to be 10 nF based on (12). The characteristic impedance (Z) of this resonant tank was calculated to be 81.64 after taking into account the values of the resonant parts. Because the characteristic impedance of the resonant tank has the potential to influence the voltage and current strains that are placed on the switches, its value should be lower than 81.64 ohms. The soft transition (ZVT) time interval may be determined by using (10), and it is around 2.8 microseconds long. This represents approximately 10% of the total switching period, which refers to when the switch is turned on and off.

Table 1. Parameters considered for the proposed converter

Parameter	Type	Value
Resonant Capacitors		4 nF
Resonant Inductors		25 μ H
Input inductor		250 μ H
Input voltage	Boost mode	100 V
Input voltage	Buck mode	200 V
Output Capacitor		470 μ F
Switching frequency		50 kHz
Duty ratio		0.5-0.6

5. SIMULATION RESULTS

The suggested converter was created by making use of MATLAB Simulink, and it was accompanied by 100 V as an input while operating in boost mode and 200 V when operating in buck mode. This converter has been put through its paces with a switching frequency of 50 kHz while producing 1.5 kW of output power. The voltage and currents of the S_a are shown in Figures 11(a) and 11(b), respectively, while the currents of S_2 and L_2 are displayed in Figures 11(c) and 11(d), respectively. The voltage of the capacitor C_2 in boost mode is displayed in Figure 11(e). The voltage and currents of the S_b are shown in Figures 12(a) and 12(b), respectively. The currents of the S_1 and L_1 are shown in Figures 12(c) and 12(d), respectively, and Figure 12(e) displays the voltage of the capacitor C_1 in buck mode. The findings that were obtained demonstrated that the predicted theoretical assumptions were correct.

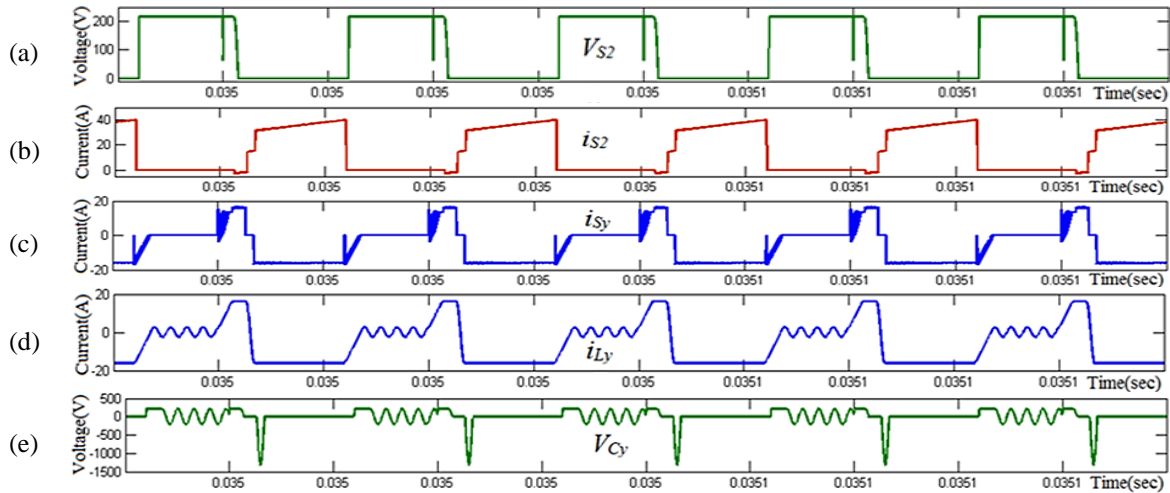


Figure 11. Simulated results (a) voltage S_2 , (b) currents of S_2 , (c) current of S_2 , (d) auxiliary resonant inductor current (L_2), and (e) auxiliary resonant capacitor (C_2) voltage: boost mode

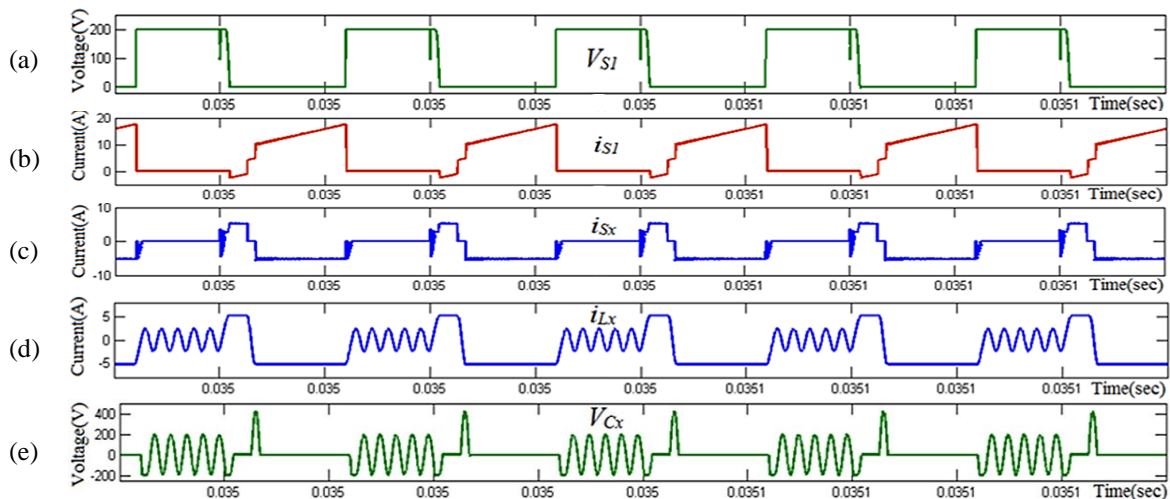


Figure 12. Simulated results (a) voltage of S_b , (b) current of S_b , (c) current of the S_1 , (d) auxiliary resonant inductor current (L_1), and (e) auxiliary resonant capacitor (C_1) voltage: buck mode

To analyze the converter's efficiency, we apply the general function of the output power to the input power. In boost mode at 70 V and 97% in buck mode at 300 V input voltage, this converter achieved an efficiency of 96.5% while operating at 400 W output power. This converter worked well with a high gain and 500 W of output power. Figures 13 and 14 show the simulated and experimental results for the efficiencies of the boost and buck modes under 800 W output power levels. Both the boost and buck modes of the converter designs have simulation efficiencies of 97.6% and 98.5%, respectively.

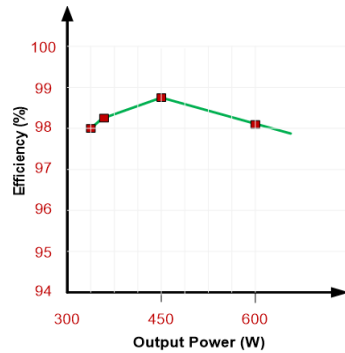


Figure 13. Boost mode efficiency curves: measured and simulated

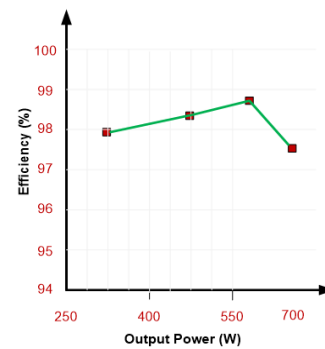


Figure 14. Buck mode efficiency curves: measured and simulated

6. CONCLUSION

A new ZVT non-isolated bidirectional DC-DC converter is presented, its working principles are described, and experimental findings are also shown in this study. To accomplish the zero-voltage transition to the main switch, the conventional converter was improved by including auxiliary parts. Reducing turn-off switching losses allowed the IGBTs to achieve soft-commutation zero current switching (ZCS). At 300 W output power, the suggested topology was 95.6% efficient in forward power transfer and 96.7% efficient in reverse power transfer, respectively, as verified by the efficiency study. Applicability to greater-power electric cars was confirmed once the suggested converter's soft-switching capabilities were confirmed. The given converter is well-suited for usage in DC traction vehicles and hybrid electric automobiles' battery storage applications because to its improved efficiency, reduced switching power losses, and reduced turn-on stresses.




REFERENCES

- [1] W. Huang and G. Moschopoulos, "A new family of zero-voltage-transition PWM converters with dual active auxiliary circuits," *IEEE Transactions on Power Electronics*, vol. 21, no. 2, pp. 370–379, Mar. 2006, doi: 10.1109/TPEL.2005.869749.
- [2] S. Dusmez, A. Khaligh, and A. Hasanzadeh, "A zero-voltage-transition bidirectional DC/DC converter," *IEEE Transactions on Industrial Electronics*, vol. 62, no. 5, pp. 3152–3162, May 2015, doi: 10.1109/TIE.2015.2404825.
- [3] M. L. Martins, H. Pinheiro, J. R. Pinheiro, H. A. Gründling, and H. L. Hey, "Family of improved ZVT PWM converters using a self-commutated auxiliary network," *IEE Proceedings: Electric Power Applications*, vol. 150, no. 6, pp. 680–688, 2003, doi: 10.1049/ip-epa:20030907.
- [4] M. R. Mohammadi and H. Farzanehfard, "New family of zero-voltage-transition PWM bidirectional converters with coupled inductors," *IEEE Transactions on Industrial Electronics*, vol. 59, no. 2, pp. 912–919, Feb. 2012, doi: 10.1109/TIE.2011.2148681.
- [5] V. V. S. K. Bhajana and P. Drabek, "A new non-isolated ZCS bidirectional Buck–boost DC–DC converter for energy storage applications in electric vehicles," *Arabian Journal for Science and Engineering*, vol. 40, no. 12, pp. 3595–3605, Dec. 2015, doi: 10.1007/s13369-015-1840-5.
- [6] H.-L. Do, "ZVS full-bridge based DC–DC converter with linear voltage gain according to duty cycle," *Journal of Electrical Engineering*, vol. 64, no. 5, pp. 331–333, Sep. 2013, doi: 10.2478/jee-2013-0049.
- [7] J. L. Russi, M. L. Martins, and H. L. Hey, "ZVT DC-DC PWM converters with magnetically-coupled auxiliary voltage source: A unifying analysis," *IEE Proceedings: Electric Power Applications*, vol. 153, no. 4, pp. 493–502, 2006, doi: 10.1049/ip-epa:20050203.
- [8] T. Mishima, S. Masuda, and M. Nakaoka, "Inductor-link open H-bridge topology-based ZCS-PWM bidirectional DC–DC converter with edge-resonant switching cells," *Electronics Letters*, vol. 51, no. 15, pp. 1191–1193, Jul. 2015, doi: 10.1049/el.2015.1174.
- [9] R. Thumma, V. V. S. K. Bhajana, P. Drabek, and M. Jara, "A new high-voltage gain non-isolated zero-current-switching bidirectional DC–DC converter," *Arabian Journal for Science and Engineering*, vol. 43, no. 6, pp. 2713–2723, Jun. 2018, doi: 10.1007/s13369-017-2702-0.
- [10] A. Elamathy, G. Vijayagowri, and V. Nivetha, "Bidirectional battery charger for PV using interleaved fourport DC-DC converter," *TELKOMNIKA Indonesian Journal of Electrical Engineering*, vol. 14, no. 3, pp. 428–433, Jun. 2015, doi: 10.11591/telkonnika.v14i3.7894.
- [11] A. Kaviani-Arani and A. Gheiratmand, "Soft switching boost converter solution for increase the efficiency of solar energy systems," *TELKOMNIKA Indonesian Journal of Electrical Engineering*, vol. 13, no. 3, pp. 449–457, Mar. 2015, doi: 10.11591/telkonnika.v13i3.7127.
- [12] T. M. Aiswarya and M. Prabhakar, "An efficient high gain DC-DC converter for automotive applications," *International Journal of Power Electronics and Drive Systems (IJPEDS)*, vol. 6, no. 2, pp. 242–252, Jun. 2015, doi: 10.11591/ijpeds.v6.i2.pp242-252.
- [13] R. G. Kumari, A. Ezhilarasi, and N. Pasula, "Control strategy for modified CI-based Bi-directional Γ -Z source DC-DC converter for buck-boost operation," *International Journal of Power Electronics and Drive Systems (IJPEDS)*, vol. 13, no. 3, pp. 1510–1518, 2022, doi: 10.11591/ijpeds.v13.i3.pp1510-1518.
- [14] O. C. Onar, J. Kobayashi, D. C. Erb, and A. Khaligh, "A bidirectional high-power-quality grid interface with a novel bidirectional noninverted buck–boost converter for PHEVs," *IEEE Transactions on Vehicular Technology*, vol. 61, no. 5, pp. 2018–2032, Jun. 2012, doi: 10.1109/TVT.2012.2192459.
- [15] M. B. Camara, H. Gualous, F. Gustin, A. Berthon, and B. Dakyo, "DC/DC converter design for supercapacitor and battery power management in hybrid vehicle applications—polynomial control strategy," *IEEE Transactions on Industrial Electronics*, vol. 57, no. 2, pp. 587–597, Feb. 2010, doi: 10.1109/TIE.2009.2025283.




- [16] Z. Zhang and K.-T. Chau, "Pulse-width-modulation-based electromagnetic interference mitigation of bidirectional grid-connected converters for electric vehicles," *IEEE Transactions on Smart Grid*, vol. 8, no. 6, pp. 2803–2812, Nov. 2017, doi: 10.1109/TSG.2016.2541163.
- [17] A. Elserougi, I. Abdelsalam, and A. Massoud, "A hybrid half-bridge submodule-based DC–DC modular multilevel converter with a single bidirectional high-voltage valve," *IET Generation, Transmission and Distribution*, vol. 17, no. 18, pp. 4146–4160, 2023, doi: 10.1049/gtd2.12974.
- [18] T. Bhattacharya, V. S. Giri, K. Mathew, and L. Umanand, "Multiphase bidirectional flyback converter topology for hybrid electric vehicles," *IEEE Transactions on Industrial Electronics*, vol. 56, no. 1, pp. 78–84, Jan. 2009, doi: 10.1109/TIE.2008.2004661.
- [19] T. V. Muni, S. V. N. L. Lalitha, B. R. Reddy, T. S. Prasad, and K. S. Mahesh, "Power management system in PV systems with dual battery," *International Journal of Applied Engineering Research*, vol. 12, no. 1, pp. 523–529, 2017.
- [20] K. Baig, K. P. Raj, G. G. R. Sekhar, T. V. Muni, and M. K. Kumar, "Power quality enhancement with active power control," *Journal of Critical Reviews*, vol. 7, no. 9, pp. 739–741, Jun. 2020, doi: 10.31838/jcr.07.09.143.
- [21] Z. Amjadi and S. S. Williamson, "A novel control technique for a switched-capacitor-converter-based hybrid electric vehicle energy storage system," *IEEE Transactions on Industrial Electronics*, vol. 57, no. 3, pp. 926–934, Mar. 2010, doi: 10.1109/TIE.2009.2032196.
- [22] S. Alatai *et al.*, "A review on state-of-the-art power converters: Bidirectional, resonant, multilevel converters and their derivatives," *Applied Sciences*, vol. 11, no. 21, p. 10172, 2021, doi: 10.3390/app112110172.
- [23] F. Z. Peng, F. Zhang, and Z. Qian, "A magnetic-less DC-DC converter for dual voltage automotive systems," in *Conference Record of the 2002 IEEE Industry Applications Conference. 37th IAS Annual Meeting (Cat. No.02CH37344)*, 2002, vol. 2, pp. 1303–1310, doi: 10.1109/IAS.2002.1042726.
- [24] A. Nasiri, Z. Nie, S. B. Bekiarov, and A. Emadi, "An on-line UPS system with power factor correction and electric isolation using BIFRED converter," *IEEE Transactions on Industrial Electronics*, vol. 55, no. 2, pp. 722–730, 2008, doi: 10.1109/TIE.2007.911199.
- [25] R. R. de Melo, F. L. Tofoli, S. Daher, and F. L. M. Antunes, "Interleaved bidirectional DC–DC converter for electric vehicle applications based on multiple energy storage devices," *Electrical Engineering*, vol. 102, pp. 2011–2023, 2023, doi: 10.1007/s00202-020-01009-3.
- [26] T. V. Muni and S. V. N. L. Lalitha, "Implementation of control strategies for optimum utilization of solar photovoltaic systems with energy storage systems," *International Journal of Renewable Energy Research*, vol. 10, no. 2, pp. 716–726, 2020, doi: 10.20508/ijrer.v10i2.10565.g7943.

BIOGRAPHIES OF AUTHORS






Prasannakumar Inampudi    has 10 years of experience in teaching. Currently, he is working as an Assistant professor at NRI Institute of Technology, Vijayawada. He did M.Tech. degree from GITAM University, Visakhapatnam, Andhra Pradesh and B.Tech. degree from SISTAM, Srikakulam, Andhra Pradesh. Presently he is pursuing his part-time Ph.D. degree at Vel Tech Rangarajan Dr. Sagunthala R&D Institute of Science and Technology, Chennai. His research areas include power systems and electric vehicles. He can be contacted at email: iprasannakumar.phd@gmail.com.



P. Chandrasekar    received a Bachelor of Technology in Electrical and Electronics Engineering from Pondicherry Engineering College, Pondicherry, in 1997, a Master of Engineering in Power Systems Engineering from the College of Engineering, Guindy, Anna University, Chennai, in 2002 and a Ph.D. degree in Electrical Engineering from Anna University, Chennai, in 2013. He has a total teaching experience of about 22 years. He has published 35 research papers in various journals and conferences at the National and International levels. H-index of 4. Five Ph.D. students are awarded degrees under his supervision. He can be contacted at email: chandrasekar1@veltech.edu.in.



Dr. T. Vijay Muni    is an Assistant Professor and researcher with more than 13 years of experience in the Department of Electrical and Electronics Engineering, at K L Deemed to be University. He received his B.Tech. degree in Electrical and Electronics Engineering from JNTU Hyderabad, M.Tech. degree in Power System and Industrial Drives from JNTUK, Kakinada, and a doctoral degree from K L Deemed to be University. He has authored 5 textbooks on electrical discipline. He has published over 52 Scopus-indexed articles, 12 Web of Science-indexed articles, and over 15 articles in peer-reviewed journals, and also published 6 patents with two grants. His areas of research include power electronic converters, energy management systems, control of electric power grids, renewable energy systems, and microgrids. He is an active Senior member of IEEE. He can be contacted at email: vijaymuni1986@gmail.com.